

DRAFT – DETC2005-xxxxx

A ROBOTIZED NEEDLE INSERTION DEVICE FOR PERCUTANEOUS PROCEDURES

Olivier Piccin, Pierre Renaud
LICIA(EA3434), INSA-Strasbourg
24, Bd de la Victoire, 67084 Strasbourg, FRANCE
Email: Olivier.Piccin@insa-strasbourg.fr

Laurent Barbé, Bernard Bayle
Benjamin Maurin, Michel de Mathelin
LSIIT (UMR CNRS-ULP 7005), Strasbourg I University
Bd. S. Brant, BP 10413, 67412 Illkirch, FRANCE
Email: barbe@eavr.u-strasbg.fr

ABSTRACT

*In this paper, a new robotized needle insertion device is proposed for computer-assisted percutaneous therapy. The device is integrated in a robotic system dedicated to gesture guidance in a Computed Tomography (CT) scan. The presented design fulfills, in an efficient way, the stringent requirements of such a medical application: compatibility with a CT-scan and a control by the practitioner through a haptic device are ensured as well as safety and sterilization are ensured. The novel design of the insertion device is first presented, outlining its main properties, before introducing preliminary experimental results.*¹

INTRODUCTION

Computed Tomography (CT) is now a widely used imaging technique for medical diagnosis as well as interventions. Thus, percutaneous procedures performed using a CT-scan for chest or abdomen treatments [?] reduce the patient trauma while ensuring the gesture accuracy of the practitioner. In such a treatment, this latter is however exposed to harmful X-rays during the needle insertion. X-ray intensity is even more harmful when CT fluoroscopy-guided intervention is achieved to improve the gesture accuracy. Providing a robotic system to remotely position and introduce the needle can therefore be an adequate solution to facilitate the use of percutaneous procedures.

CT-guided surgery systems have already been proposed. The RCM+PAKY system [?, ?, ?] has been efficiently used in the operating room. Clinical experiments [?, ?] have also been achieved in other medical fields, that validate the computer-aided

surgery by needle insertion. In these systems, image-guided positioning has been proposed. Nevertheless, no haptic feedback is given to the practitioner, whereas his gesture depends strongly on the evaluation of the needle insertion force. Furthermore, breath compensation is not considered and seems delicate to take into account, while it is of great importance for chest or abdomen applications.

As a consequence, we currently develop a robotized CT-guided needle insertion system with haptic feedback : a needle positioning robot has been developed [?] which is compatible with the CT-scan, and can be fastened to the patient to avoid the influence of the breath. The needle positioning robot is based on a 5-dof parallel structure to set the position and orientation of the needle. A stereotactic system enables us to locate the target of the treatment with respect to the robot using only one CT-scan image [?]. The stiffness of the structure is enhanced due to the parallel architecture, and compactness is optimized so that a standard CT-scan can be used for the intervention.

To our knowledge, very few papers have been published about the design of a robotized needle insertion device to control the penetration of the needle. Friction-based insertion devices have been proposed in [?, ?]. The main interest is the large needle stroke: since its displacement is obtained by a continuous rotation movement, the system compactness is ensured. The use of friction also enables the authors to mechanically limit the insertion effort, since no haptic feedback is given to the practitioner. In our currently developed robotic system, the needle displacement must be, on the contrary, evaluated to give the surgeon the needle tip position as well as the insertion effort. A new robotized needle insertion device is therefore proposed fulfilling the

¹This draft paper contains proprietary intellectual property of the authors.

requirements of a remotely force-controlled needle insertion, the compactness needed to use a standard CT-scan, as well as safety and sterilization requirements due to the medical context.

In the second section, the overall structure of the needle positioning robot is briefly recalled. The design of the proposed needle insertion device is then presented, outlining its kinematic properties and the thorough adequacy with the medical requirements. In the fourth section, current development of the prototype is described and a first validation of the proposed architecture is demonstrated through preliminary experimental results. Conclusions on further developments of the insertion device and the overall robotized system are finally drawn.

THE ROBOTIZED PERCUTANEOUS THERAPY SCENARIO

In this section, the overall structure of the needle positioning robot is briefly recalled, with the associated intervention procedure, to outline the design requirements of the needle insertion device. Further details may be found in [?, ?, ?].

The Robotic Positioning Device

The needle positioning robot called CT-Bot is a parallel mechanism attached to the abdomen of the patient with special straps. Its size is less than 200 mm high, 250 mm large and 200 mm depth. It weighs less than 2.5 kg which is suitable for every kind of patient. This mechanism features five degrees of freedom required to position the needle and orient the line supporting its axis. Figures 1 and 2 show the CAD model of the CT-Bot and a constructed prototype.

The structure is composed of one 6-bar linkage and a 4-bar linkage joined together by the end-effector. Due to the choice of the legs geometry, the forward and inverse kinematic models can be computed analytically.

The positioning of the end-effector is obtained using ultrasonic motors. The high holding torque of these motors fits particularly the safety requirements in this medical application: the needle positioning robot remains stable in case of accidental power failure.

The Robotized Percutaneous Procedure

Once a percutaneous therapy is decided by the practitioner, the procedure is composed of three main steps:

1 - Registration of the Robot with Respect to the Patient. The robot registration is performed using a specifically developed marker linked to the base of the robot. From one CT-scan image of this marker, the robot base position and orientation can be computed [?], which enables us to estimate the target position with respect to the robot. This registration is

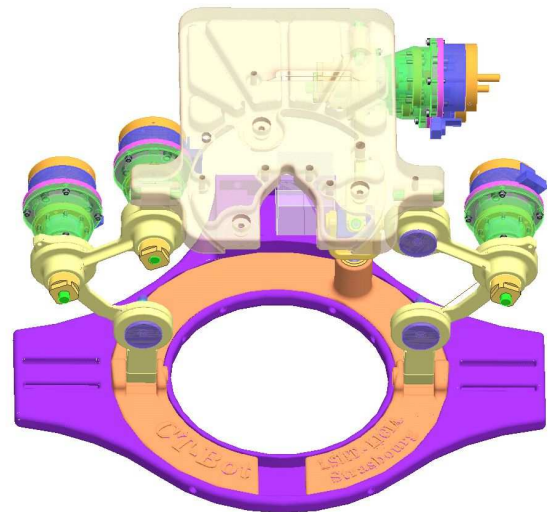


Figure 1. CT-BOT CAD MODEL.



Figure 2. CT-BOT PROTOTYPE.

well adapted to the fact that a CT-scan only provides image slices which are about 20mm thick. One must notice that the needle tip is therefore likely to be invisible in the image plane for many robot positions. It is therefore necessary to estimate the tip position with respect to the robot using the needle insertion device.

2 - Displacement of the Needle Positioning Robot.

From the previous registration, the robot end-effector can be positioned for the insertion procedure. The positioning is performed using a real-time collision avoidance algorithm so that the device configuration is always valid.

3 - Force-Controlled Needle Insertion Using Haptic Feedback. When the robot end-effector position and orientation are obtained, the needle insertion can be performed. The

practitioner uses the visual feedback through the CT-scan image to estimate the needed displacement and the insertion effort to get information on the nature of the tissues. The self-rotation of the needle is also needed to orient the needle's bevel.

The needles have a size which varies from 100 to 180 mm in length and 0.5 to 2.4 mm in diameter. The available space to carry out insertion is limited by the size of the ring of the scanner and the patient's corpulence. The minimal available volume corresponds to a 200 mm radius half-sphere centered on the entry point of the needle. A main constraint of the insertion device is therefore its compactness.

Finally, in this robotized percutaneous therapy scenario, the needle insertion device needs to provide:

1. two degrees-of-freedom, the needle insertion displacement and its self-rotation
2. the insertion force measurement to provide the practitioner with a force feedback through a haptic device
3. an insertion principle compatible with the small available volume in the CT-scan, and which allows us also to locate the needle tip with respect to the robot end-effector
4. safety and sterilization properties

DESIGN OF THE INSERTION DEVICE

In this section, the main elements of the insertion device are presented to outline its integration to the existing needle positioning robot. The device design is then detailed, before introducing the needle kinematics, the insertion force measurement principle and the device compatibility with medical requirements.

Global Overview

The main components of the needle insertion device are presented on the figure 3 with the platform of the previously developed needle positioning robot (item 1 on the figure). The device is composed of three parts: the interface supporting the sensors for needle insertion force measurement (item 2), the driving mechanism including the actuators for all the needle displacements (item 3) and the needle insertion mechanism that performs both grip and displacements of the needle (item 4).

Design presentation

Gripping of the Needle. The gripping of the needle is carried out using two specifically-designed miniature chucks allowing the insertion device to grasp needles with various diameters. Each chuck is composed of a body, three jaws, a spur gear and an indexing ring (Figure 4). The rotation of the gear *wrt* the body generates a radial displacement of the jaws and consequently the grasp or release of the needle.

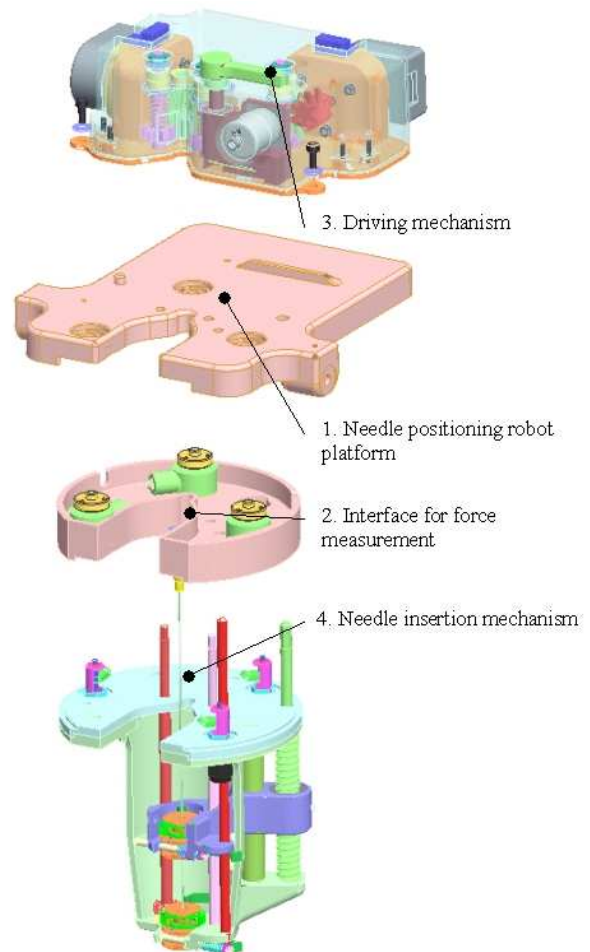


Figure 3. EXPLODED VIEW OF THE NEEDLE INSERTION DEVICE.

Insertion Mechanism Design. The insertion mechanism is composed of a casing and a mobile carriage in translation *wrt* the casing (Figure 5). A chuck C_1 is mounted on the casing while the other C_2 is linked to the carriage. This latter is displaced by means of the shaft 1 thanks to a nut. The tightening/release of the chucks C_1 and C_2 is obtained by the rotation of the shafts 2 and 3.

For each chuck, a pawl system controls the rotation of the indexing ring so that the chuck self-rotation is blocked during a needle release. On the opposite, the chuck and the needle can turn simultaneously during a needle tightening if the applied torque is beyond a threshold defined by the pawl system design.

The two chucks are locked in position using two stems 1 and 2 (Figure 5). These stems are pushed in release position by two compression springs so that a rotation of the shaft 4 induces the extraction of the chucks.

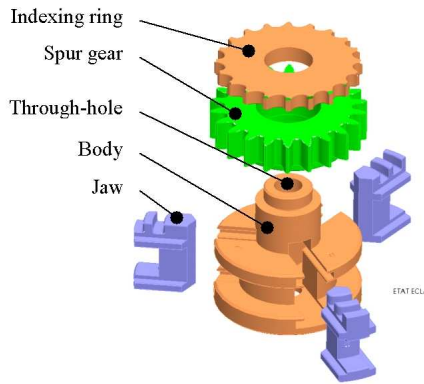


Figure 4. EXPLODED VIEW OF A CHUCK.

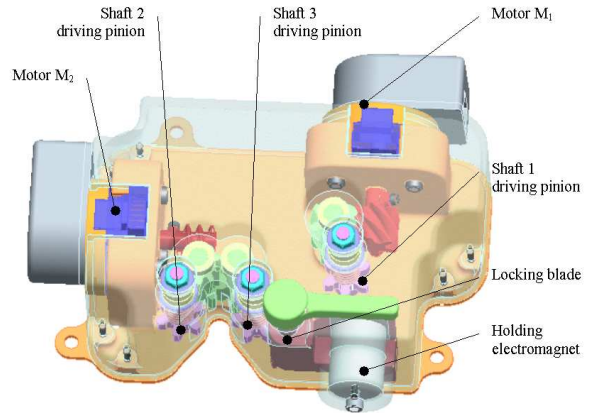


Figure 6. DRIVING MECHANISM.

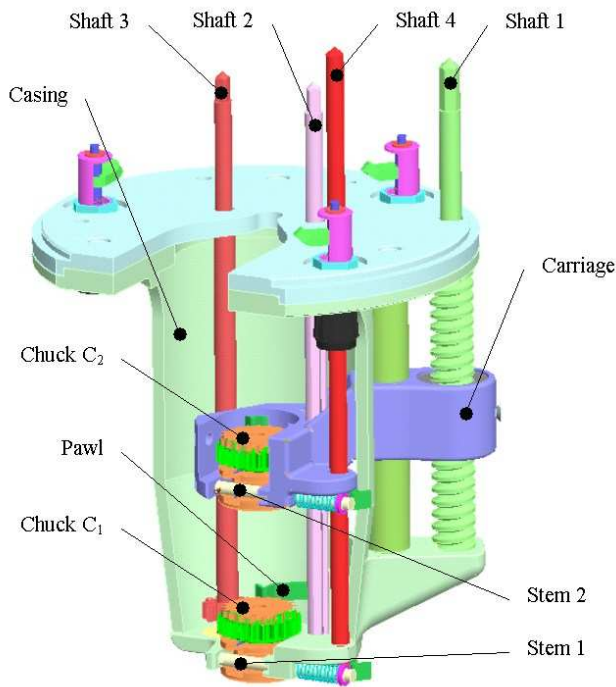


Figure 5. INSERTION MECHANISM.

Driving Mechanism Design. The driving mechanism is composed of two piezoelectric ultrasonic motors M_1 and M_2 (Figure 6). The shaft 1 is actuated by the motor M_1 for carriage translation. The motor M_2 drives simultaneously in rotation the shafts 2 and 3 with opposite directions, thanks to a special gear arrangement. The rotation of only one actuator operates therefore the simultaneous tightening of one chuck (for example C_1) and the loosening of the other (C_2).

A spring-pulled locking blade is maintained armed by a controlled holding electromagnet. In case of power failure, the hold-

ing effort vanishes and the locking blade swivels of a fraction of turn. In this way, it drives the shaft 4 in rotation which itself causes the release of the stems 1 and 2.

Device Kinematics

Needle Translation. To perform the large needed needle translation in the limited available volume, the translational movement is split into a sum of elementary translations. These elementary displacements are obtained using translation of the carriage and alternate tightening of the chucks (figure 7).

Initially, the carriage is in its upper position and the chuck C_2 is tightened on the needle. The needle guidance is ensured by having the jaws of the lower chuck C_1 in loose contact with the needle (figure 7-a).

The insertion movement cycle breaks up then into four steps :

1. The carriage is translated to its lower position (figure 7-b)
2. The chuck C_2 is loosened while C_1 is tightened on the needle (figure 7-c)
3. The carriage is translated to its initial position. The needle position remains constant due to its grasp with the chuck C_1 (figure 7-d)
4. The chuck C_2 on the carriage tightens whereas the lower prehensor C_1 releases the needle (figure 7-e).

This cycle is iterated until the needle tip is at the desired position. For needle extraction, the movement breaks up similarly except that the carriage stands initially in its lower position.

Needle Rotation. As previously presented, the pawl systems installed on the chucks limit the tightening torque applied to the needle. Beyond a given torque threshold, the tightened chuck can rotate with the needle providing in this manner a security against overloading.

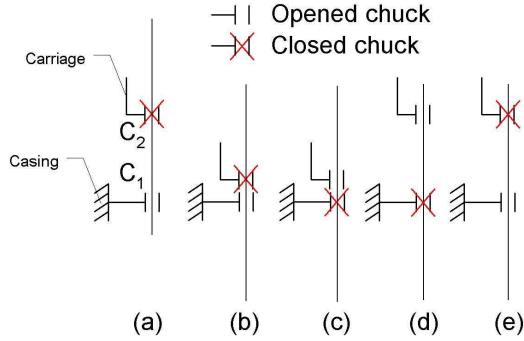


Figure 7. INSERTION CYCLE.

It should therefore be noted that the single motor M_2 not only performs the needle tightening/release but then also allows the practitioner to rotate the needle about its axis. As a result, the proposed system features a needle self-rotation capability useful for the surgeon to modify the bevel's orientation without an additional actuator.

Insertion Force Measurement

The interface 2 (Figure 3) is connected to the platform of the needle positioning robot by three unidirectional force sensors (A_1, A_2, A_3) symmetrically placed on a circle of radius r drawn around the needle axis (Figure 8). Vector $\vec{\#}_z$ indicates the needle axis which is different from the direction of gravity $\vec{\#}_0$ (not represented on figure 8). The entry point on the patient's skin is B located at a distance d from the plane (A_1, A_2, A_3). The z -component of the effort $\vec{\#}_{S \rightarrow N}$ exerted by the skin (S) on the needle (N) can be computed from the forces m_1, m_2 and m_3 measured by the three sensors as follows :

$$\vec{\#}_{S \rightarrow N} \cdot \vec{\#}_z = Mg \vec{\#}_0 \cdot \vec{\#}_z - m_1 - m_2 - m_3 \quad (1)$$

where M and $-g \vec{\#}_0$ denote the mass of the insertion mechanism attached to the robot's platform and the gravity acceleration. The platform orientation remains constant during the insertion so that $Mg \vec{\#}_0 \cdot \vec{\#}_z$ is a measurement offset easily identified before the needle penetration.

The special arrangement of uniaxial sensors enables us also to calculate two components of the torque exerted by the skin to the needle, expressed at point O :

$$\vec{M}_{O,S \rightarrow N} \cdot \vec{\#}_x = Mg \vec{OG} \wedge \vec{\#}_0 \cdot \vec{\#}_x - \frac{r}{2} m_2 - \frac{r\sqrt{3}}{2} m_3 \quad (2)$$

$$\vec{M}_{O,S \rightarrow N} \cdot \vec{\#}_y = Mg \vec{OG} \wedge \vec{\#}_0 \cdot \vec{\#}_y + r m_1 - \frac{r\sqrt{3}}{2} m_2 - \frac{r}{2} m_3 \quad (3)$$

where G denotes the center of mass of the insertion mechanism.

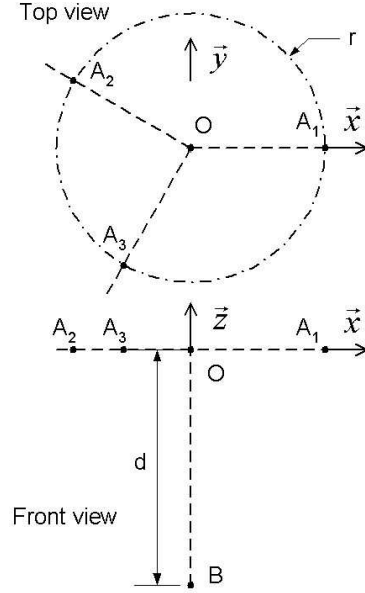


Figure 8. SCHEMATIC REPRESENTATION OF FORCE SENSORS LOCATION.

These information on the torque applied to the needle can be useful for control purposes to detect lateral flexure under needle insertion loading.

Medical Requirements

With the proposed design, the robotized insertion device exhibits several safety properties. First, the gripping of the needle and its displacement are completely decoupled from a kinematic point-of-view and operated by non-backdrivable transmissions. The control of the system is hence simplified and the needle tip position is not influenced by interaction with the environment. Furthermore, the use of ultrasonic motors enhances safety in the event of a power failure since the configuration of the needle driver remains unchanged. Finally, the chucks linked to the needle can be extracted at any time during the needle insertion or extraction, thanks to the holding electromagnet located on the driving mechanism. The robotic system can therefore be disengaged in a few seconds if needed for medical reasons.

Concerning the sterility requirement, it must be noticed that the proposed needle insertion device breaks up into two main parts. The active part of the system comprising the force sensors and the driving mechanism is attached to the robot's platform. The robot and the active part of the needle insertion device can be wrapped in a sterile bag whereas the passive part corresponding to the needle insertion mechanism can be easily detached and sterilized. The chucks constructed out of polycarbonate can also be sterilized and used as disposable units.

CURRENT DEVELOPMENT AND PRELIMINARY EXPERIMENTS

In this section we present the current state of development of the needle insertion device. A first prototype has been produced to achieve some preliminary experiments concerning the CT-scan compatibility and the tightening capability of the chucks.

Current Development

The first release of a prototype has been constructed to validate the presented design. Most of the parts have been obtained using a rapid prototyping system excepting the threaded shaft 1 that has been machined with conventional means (Figure 10). In the same way, the chuck physical properties needed to be close to the final-product ones. A mold has therefore been constructed using rapid tooling to produce chucks in polycarbonate (Figure 9).

Due to their small size, mechanisms such as the pawl systems and the quick needle release feature are still in development.

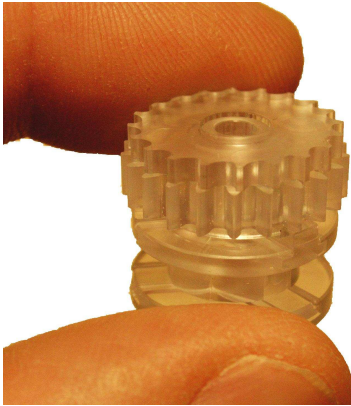


Figure 9. FABRICATED PROTOTYPE OF A CHUCK.

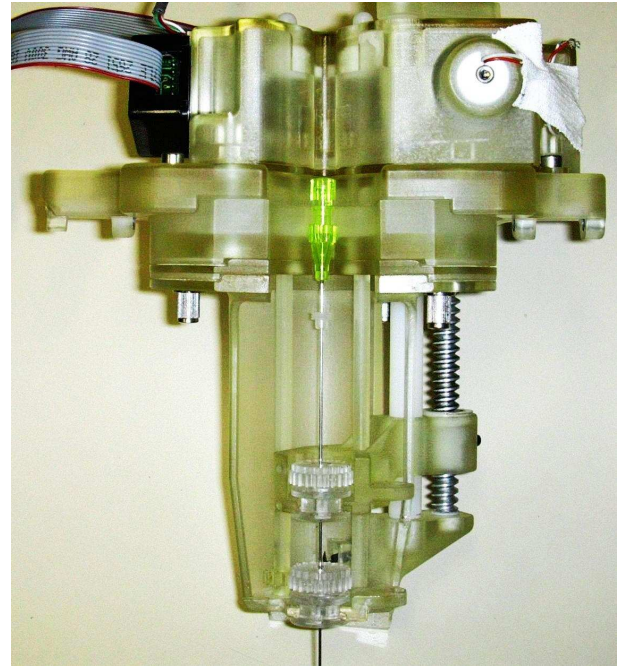


Figure 10. FABRICATED PROTOTYPE OF THE INSERTION DEVICE.

CT-Scan Compatibility

Some experiments have been performed at the University Hospitals of Strasbourg to perform “point-to-click” trials on a phantom. Figure 11 shows a DICOM image acquired from the CT-scan with the needle positioning robot equipped with the insertion device. During this experiment the overall system demonstrated a correct radiolucency : almost all the needle barrel is visible in the image.

Needle Tightening Capability

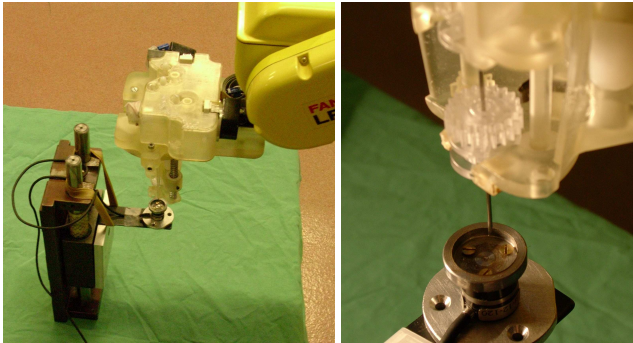
Previous experiments [?] have shown that a robotized insertion device must be able to apply efforts in the order of 10 N.



Figure 11. CT-SCAN IMAGE OF THE ROBOTIC SYSTEM.

Experiments have been achieved to validate the currently developed prototype behavior, and especially the absence of needle sliding in the chucks.

The experimental set-up is composed of the insertion device, a needle, an ATI Nano-17 six axis force sensor, a PC for data acquisition, a spring-pulled cart sliding on two columns and a six DOF robot FANUC LR-200i (Figure 12). The needle and the insertion device are linked to the robot, and displaced at a



(a) Global View

(b) Close-Up

Figure 12. EXPERIMENTAL SETUP FOR NEEDLE INSERTION EFFORT CAPABILITY.

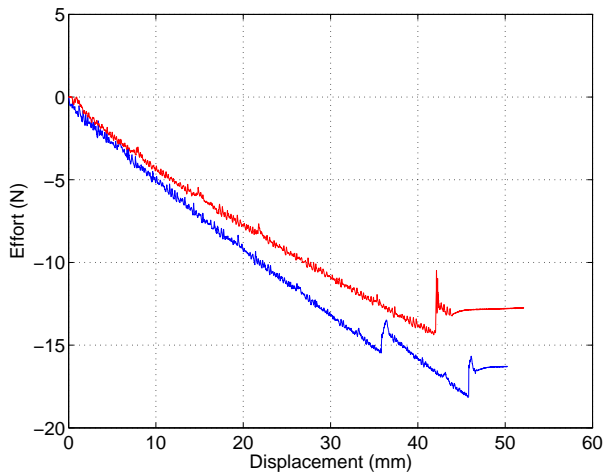


Figure 13. EFFORT MEASUREMENT DURING THE NEEDLE DISPLACEMENT (UPPER CURVE: 0.72mm NEEDLE, LOWER CURVE: 1.27mm NEEDLE) - NEGATIVE VALUES ARE DUE TO THE COMPRESSION EFFORT OF THE NEEDLE TIP ON THE FORCE SENSOR.

constant speed of 1 mm/s .

Thanks to the spring-pulled cart, the position control of the needle tip achieved with the robot must be equivalent to a force control of the effort applied on the needle tip. Using a velocity-controlled needle displacement, the effort measured with the force sensor in contact with the needle tip must therefore vary regularly. Discontinuities in the force/displacement relationship are due to sliding in the chuck.

No needle sliding is observed for an effort below 10 N for the two tested needles of 1.27 mm and 0.72 mm diameters. The maximum efforts are equal to 15.5 N and 14.5 N for respectively the 1.27 mm and 0.72 mm needles. The deviation between the two curves seems to be due to the flexure of the needles, which

does not influence the experimental results. This first evaluation of the needle tightening capability of the insertion device tends to validate the proposed design.

CONCLUSION

In this paper, a new insertion needle device has been proposed. This device is included in a robotic system dedicated to gesture guidance in percutaneous procedures.

A grasp/release scheme has been proposed to accommodate various sizes of needles and to allow force sensors integration for haptic feedback. The specific kinematics ensures the device compactness required for use in a CT-scan without introducing redundant actuation since two motors control the two required DOF. Needle displacements are controlled in a safe way and the system architecture facilitates its sterilization.

The first release of a prototype has been issued for preliminary experiments. Further evaluations will be performed on a bench and in a CT-scan to validate the design. The development of the robotic system will then include the design of a specific haptic interface to interact with the surgeon.

ACKNOWLEDGMENT The authors wish to thank the Alsace Region and the CNRS-ROBEA program for the financial support of this research work.